Measurements of Wall Permittivity and Target Radar Cross Section for Through-the-Wall Radar Imaging System Design

S. Pisa(*), E. Pittella(*), E. Piuzzi(*)
P. D'Atanasio(**), A. Zambotti(**)

(*) SAPIENZA UNIVERSITÀ DI ROMA — Department of Information Engineering, Electronics and Telecommunications (DIET)

(**) ENEA Italian National Agency for New Technologies, Energy and Sustainable Economic Development — Casaccia Research Center

Outline

- Through-the-Wall Radar Imaging (TWRI) Systems
- Wall Permittivity Measurements
- Radar Cross Section Measurements
- TWRI Results

Through-the-Wall Radar Imaging Systems

Through-the-Wall Radar Imaging Systems

General characteristics

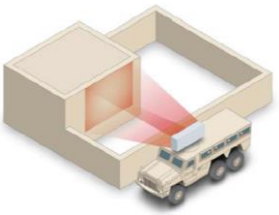

- Through-the-wall radar imaging (TWRI) allows police, fire personnel, and defense forces to detect, identify, and track the whereabouts of humans and moving objects inside buildings.
- **PRIN 2015 Project U-VIEW (Ultra-wideband Virtual Imaging Extra Wall for high-penetration high quality imagery of enclosed structures).**
- **University of Genova**
- **University of Calabria**
- **Sapienza University of Rome**
- **University of Rome 3**

Through-the-Wall Radar Imaging Systems

Review of proposed apparatus

Proponent	General system description	Technical data	Antennas	Reconstruction algorithm
Lincoln Laboratory (MIT)	FMCW Radar.	2-4 GHz frequency band. 1 W peak power.	Multiple-Input, Multiple-Output (MIMO). 13 TX and 8 RX Vivaldi plus linear slot antennas.	Range migration algorithm (RMA) synthetic aperture radar (SAR) technique.
French Aerospace Lab.	FMCW Radar.	2-4 GHz frequency band. 17 dBm output power.	MIMO. 4 TX and 8 RX antennas.	Numerical model of the overall radar system.
US Army Research Laboratory (ARL)	Ultra Wideband (UWB) Radar.	0.3-3 GHz frequency band. 5 mW average power.	2 TEM horns as TX antennas and 16 Vivaldi as RX antennas.	Back projection algorithm.
Villanova University, Pennsylvania,	Stepped Frequency Radar (SFR).	1-3 GHz frequency band.	MIMO. 2 horn TX antennas. A moveable RX horn antenna.	Compressive sensing (CS) technique.
Massachusetts Institute of Technology	FMCW radar.	5.46 and 7.24 GHz frequency bands.	T-shaped antenna array vertical segment TX antennas, horizontal segment RX antennas	Software able to reconstruct various human body parts at different time steps and stitch them together to capture a moving human figure.

Through-the-Wall Radar Imaging Systems

Experimental set-up (SFR) (Multi-frequency, Multi-modality)

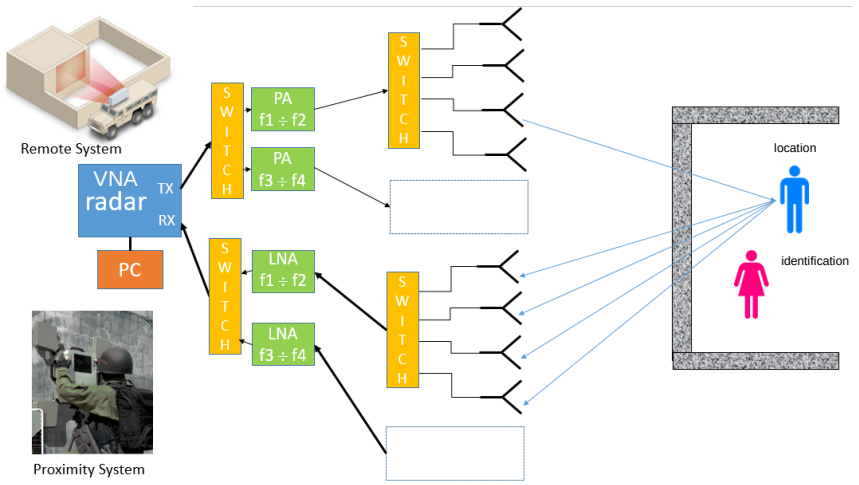

Through-the-Wall Radar Imaging Systems

TX-RX Antennas of the TDM MIMO radar system

The radar uses a subset of all possible antenna combinations, which consist of 44 bistatic antenna element combinations whose effective phase centers approximate a linear array evenly spaced λ/2

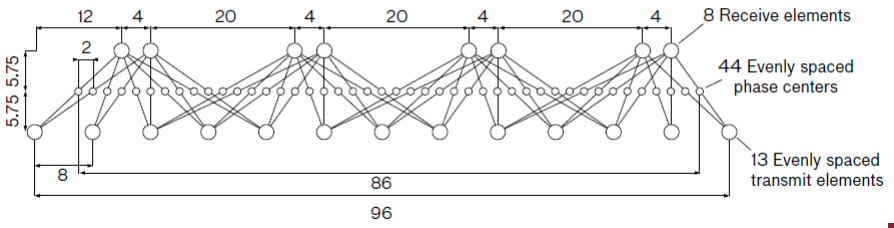

Through-the-Wall Radar Imaging Systems

Simplified Scenario

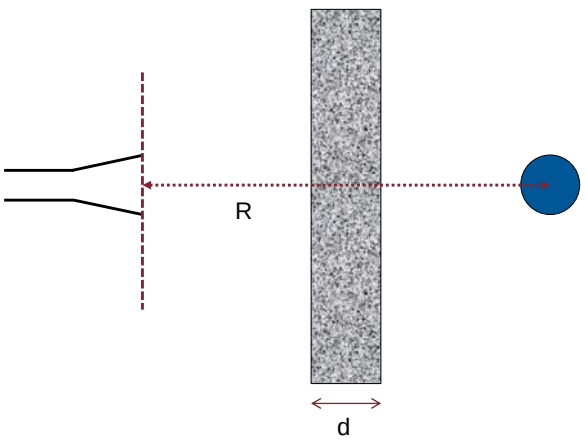

Through-the-Wall Radar Imaging Systems

Design Equation (Radar Equation)

$$\frac{P_r}{P_t} = \sigma(f)|T(f|^4 \frac{G(f)^2}{4\pi} \times \left(\frac{\lambda}{4\pi R^2}\right)^2$$

- P_r , P_t = Received and Transmitted Power
- λ = free space wavelength
- σ = Target Radar Cross Section (RCS)
- T = Wall transmission coefficient
- G = Antenna gain
- R = Antenna Target distance

Through-the-Wall Radar Imaging Systems

Radar Cross Section (RCS)

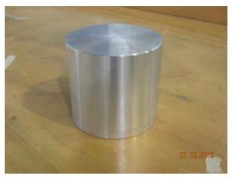

ϕ =12.8 cm, h=12 cm

$$\sigma = \lim_{r\to\infty} 4\,\pi\, r^2 \frac{|E_s|^2}{|E_i|^2}$$

where E_s and E_i are the scattered and incident electric field intensities

Through-the-Wall Radar Imaging Systems

TWRI Inversion algorithms:

Simulations inside Microwave Studio by CST

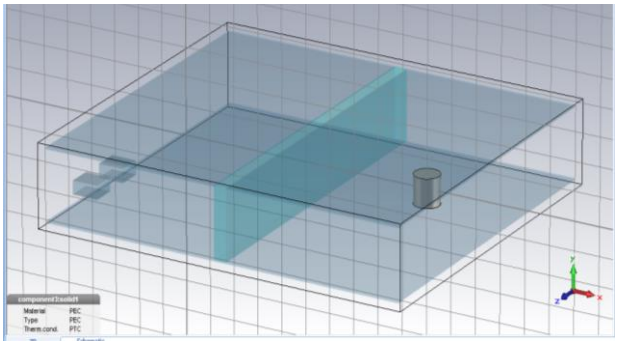

The S21 scattering parameters between TX and RX antennas are computed for various antenna positions

Wall Permittivity Measurements

Systems for permittivity measurement
Standard wideband high-frequency solutions

- Open-ended coaxial probe
  - The probe tip is placed in contact with the material under test
  - Permittivity is retrieved from the reflection coefficient measured at the probe connector

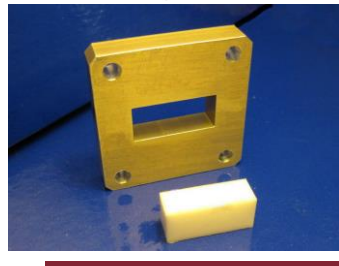

- Waveguide system
  - The material under test is embedded in a length of waveguide
  - Permittivity is retrieved from the reflection and transmission coefficients measured at the flange ports

Systems for permittivity measurement
Review of Literature Data

MATERIAL	Frequency Range	ε_r'	ε_r''
CONCRETE	10 MHz – 1 GHz	4.6	0.1
CONCRETE	3 GHz – 24 GHz	7 ÷ 5	0.1 ÷ 0.2
BRICK	3 GHz – 24 GHz	3.6 ÷ 4.6	0.12 ÷ 06
STONES		≅ 6	
GLASS	9.4 GHz	4	$5.0 \cdot 10^{-4}$
WOOD		1.2 ÷ 6.8	0.006 ÷ 0.43

Proposed measurement system
Free-Space Systems

- For standard systems, the sensitive volume is small, while building walls are an extremely heterogeneous material with a rather coarse grain.
- Testing of a large piece of wall is mandatory in order to achieve significant results.
- **⇒ free-space system based on a Vector network analyzer (Agilent PNA-L N5230A) and measurement software (Agilent 85071E) and a couple of aperture antennas**
- **⇒ truncated waveguide antennas, suitable to cover the desired frequency range (1 – 8 GHz): WR-650 (1 – 1.7 GHz); WR-430 (1.7 – 2.6 GHz); WR-284 (2.6 – 4 GHz); WR-187 (4 – 6 GHz); WR-137 (6 – 8 GHz)**

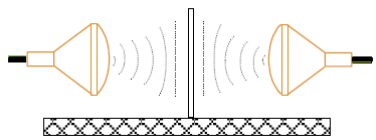

Proposed measurement system
Measurement model

- The adopted measurement model, developed by NIST, uses as input quantities the scattering parameters at the sample surfaces

$$|S| = S_{11}S_{22} - S_{21}S_{12} = \frac{\Gamma^2 - T^2}{1 - \Gamma^2 T^2}$$

$$T = e^{-\gamma L}$$

$$\gamma = j\,\frac{2\,\pi\,f\,\sqrt{\varepsilon_r^*}}{c}$$

$$\Gamma = \frac{1 - \sqrt{\varepsilon_r^*}}{1 + \sqrt{\varepsilon_r^*}}$$

- The complex permittivity value ε_r^* is evaluated by **minimizing the least-square difference between the measured scattering parameters and the theoretical values predicted by the Eqs.**
- The scattering parameters must be measured at the sample surfaces, which requires a suitable de-embedding and **error-correction procedure**

Proposed measurement system
SOLT vector error correction procedure

- The parameters of the “error network” are evaluated through measurements on four known standard loads (**S**hort, **O**pen, matched **L**oad, **T**hrough) with the Agilent 85032F N-type mechanical SOLT calibration kit.
- The standards are applied at the coax terminals that will be connected to the antennas
- Errors from cables and connectors are evaluated and then removed

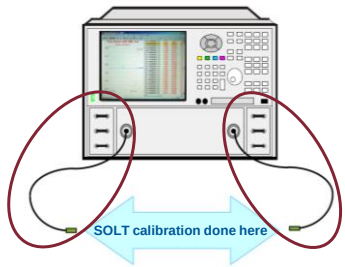

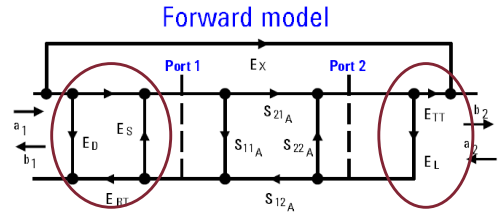

E_D = fwd directivity
E_S = fwd source match
E_{RT} = fwd reflection tracking
E_L = fwd load match
E_{TT} = fwd transmission tracking
E_X = fwd isolation

Proposed measurement system
Gated-Reflect-Line:

Time Domain Gating

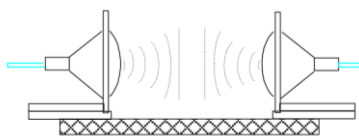

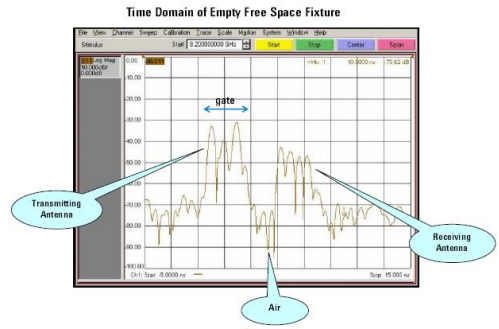

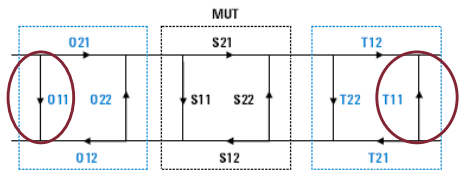

- **Time Domain Gating Evaluates Directivity Errors O11, T11**

Proposed measurement system

GRL: vector error correction procedure

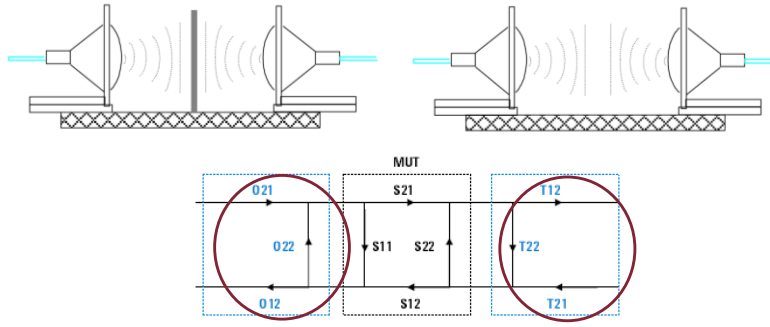

- **The metal plate (Reflect) and a Thru (Line) measurement, evaluate the remaining four Error Parameters. The reflect measurement is performed with two flat metallic panels placed in contact with the two surfaces of the wall under test.**

Proposed measurement system

Metrological analysis: measurement set-up

polymethyl methacrylate **(PMMA), better known as Plexiglas®**

Open site

Anechoic chamber

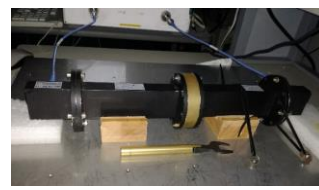

WR-187 Waveguide

Proposed measurement system

Metrological characterization: PMMA measurements

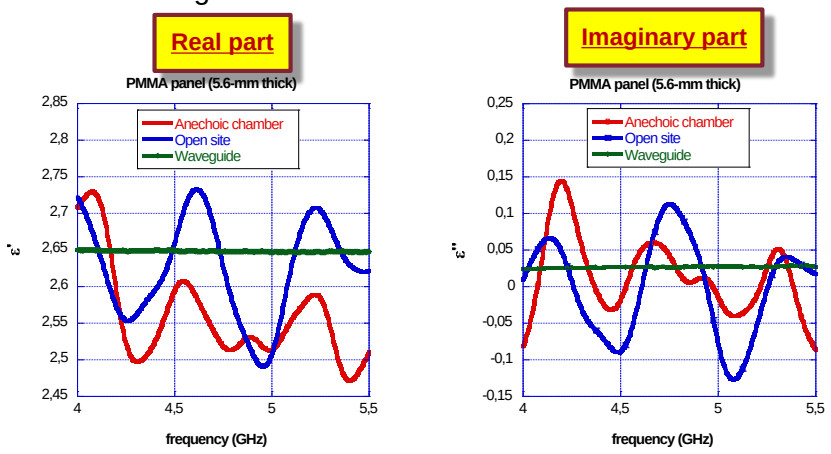

S. Pisa, E. Pittella, E. Piuzzi, P. D'Atanasio, A. Zambotti, "Permittivity measurement on construction materials through free space method", Proc. I2MTC Torino, May 22-25 2017, pp. 1225-1228

Proposed measurement system

Metrological characterization: results on PMMA

	Waveguide	Open site	Anechoic chamber
Real part average	2.6482	2.62	2.56
Real part std. dev.	0.0009	0.07	0.07
Imaginary part average	0.026	–	–
Imaginary part std. dev.	0.001	–	–

- **Better performances of the waveguide system with percentage variations of 0.03% as compared to the 3% value of the free space systems**
- **Performances are rather poor in measuring the imaginary part of the permittivity, mainly due to the low losses of the test material.**

Proposed measurement system
Theoretical uncertainty analysis: expanded uncertainty

- Combined uncertainty from NIST measurement model

$$\frac{\Delta\varepsilon'}{\varepsilon'} = \frac{1}{\varepsilon'}\sqrt{\sum_{\alpha}\left[\left(\frac{\partial\varepsilon'}{\partial|S_\alpha|}\Delta|S_\alpha|\right)^2 + \left(\frac{\partial\varepsilon'}{\partial\theta_\alpha}\Delta\theta_\alpha\right)^2\right] + \left(\frac{\partial\varepsilon'}{\partial L}\Delta L\right)^2}$$

- The first uncertainty contribution depends on instrumental uncertainty related to scattering parameters measurements
- The second uncertainty contribution depends on sample length (measured by using a caliper with 0.02 mm resolution) measurement uncertainty
- **Instrumental uncertainty** is about **5%** in **test measurements on PMMA**, while the contribution due to **uncertainty in sample length** is **negligible**
- **Typical uncertainty in free-space measurements with Agilent 85071E material measurement software (as stated by the manufacturer): 2 – 3%**
- **The above calculated uncertainty figures match well with the observed variations in the measured permittivity in open site and anechoic chamber**

Proposed measurement system
Realistic example: travertine wall

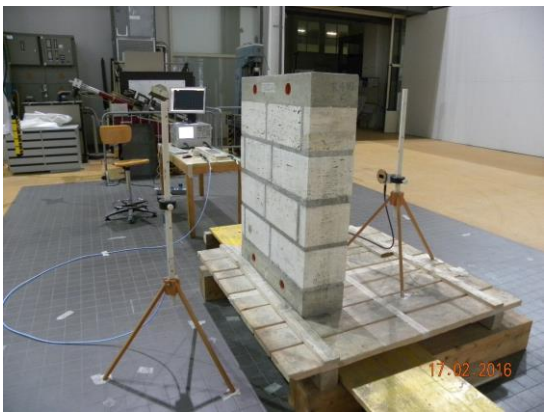

- The nature of the material affects measurement uncertainty because of the following effects:
  - **The greater thickness mitigates the effect of instrumental uncertainty (which decreases to about 3%)**
  - **The greater uncertainty in the measurement of the sample length introduces a second relevant contribution, equal to about 4%**

Proposed measurement system

Realistic measurements: results on different kinds of walls

Real part of permittivity

Type of wall	Average value	Repeatability
Travertine	6.02	0.05
Brick	3.82	0.04
Tuff	3.78	0.03

Radar Cross Section

RCS
Review of literature data

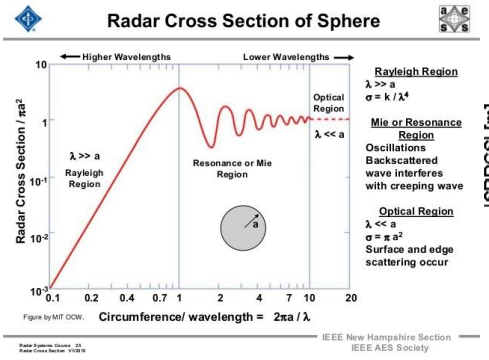

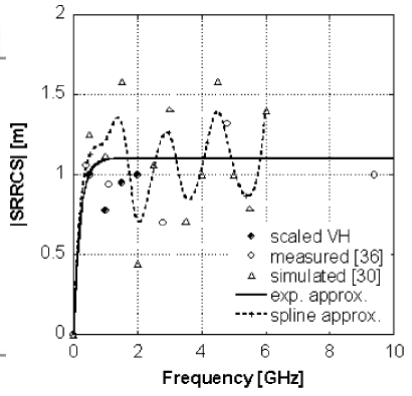

S. Pisa, P. Bernardi, M. Cavagnaro, E. Pittella, and E. Piuzzi, "A circuit model of an ultra wideband impulse radar system for breath-activity monitoring," Int. J. Numer. Model., vol. 25, 46-63, 2012.

RCS Measurements
Anechoic chamber

E. Piuzzi, P. D'Atanasio, S. Pisa, E. Pittella, and A. Zambotti, "Complex radar cross section measurements of the human body for breath activity monitoring applications," *IEEE Transactions on Instrumentation and Measurement*, vol. 64, no. 8, pp. 2247- 2258, August 2015.

RCS Measurements

RCS equations

$$|\sigma_{\text{tgt}}| = |\sigma_{\text{ref}}| \frac{|S_{11\text{tgt}} - S_{11\text{empty,tgt}}|^2}{|S_{11\text{ref}} - S_{11\text{empty,ref}}|^2}$$

$$\text{angle}(\sigma_{\text{tgt}}) = \text{angle}(\sigma_{\text{ref}}) + \text{angle}(S_{11\text{tgt}} - S_{11\text{empty,tgt}}) - \text{angle}(S_{11\text{ref}} - S_{11\text{empty,ref}})$$

- The empty chamber (without target) background trace ($S11_{empty}$) is acquired and subsequently subtracted from the target trace ($S11_{tgt}$)
- This allows to compensate for unwanted reflections from the environment and the antenna itself
- The RCS of the actual target under investigation is then derived by comparison with the calibration target response.

RCS Measurements

RCS of a Cylinder (12.8 cm diameter, 12 cm Height) Flat panel as ref.

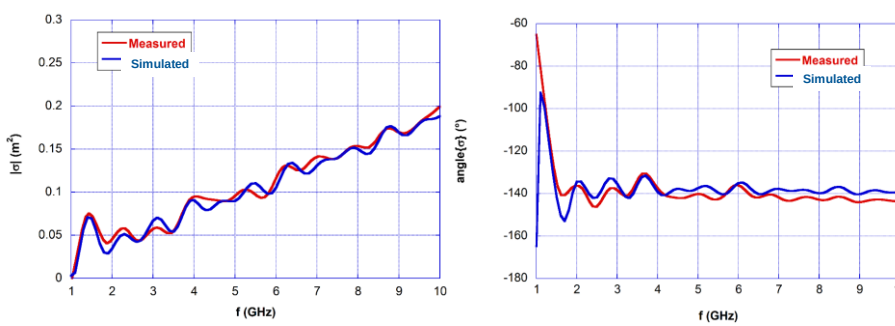

Simulated = FEKO. The maximum error on the magnitude of the measured RCS is 1 dB, while the corresponding maximum error on the angle is 5° .

RCS Measurements

Theoretical uncertainty figures

RCS MAGNITUDE UNCERTAINTY BUDGET

Uncertainty contribution	dB
1. Pointing error	0.3
2a. Cross-polarization error (calibration target)	0.1
2b. Cross-polarization error (verification target)	0.1
3. Nonlinearity	0.3
4. Range	0.1
5. Reference RCS	0.2
6a. Background subtraction (calibration target)	0.5
6b. Background subtraction (verification target)	0.5
Overall uncertainty (RSS)	**1.0**

The overall theoretical uncertainty, obtained as a **root-sum-square (RSS)** uncertainty, of 1.0 dB is perfectly compatible with the experimentally verified uncertainty.

RCS Measurements

RCS of a volunteer

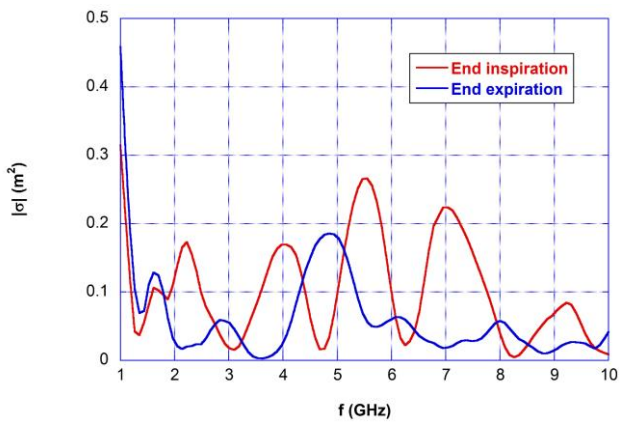

The two traces clearly evidence that the absolute value of the RCS is greatly influenced by the small movements of the human thorax wall resulting from respiratory acts.

TWRI Results

Feasibility Study

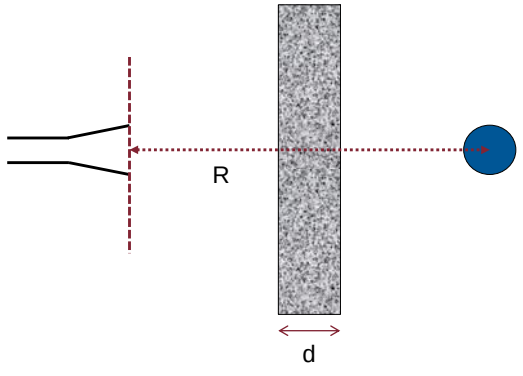

$$\frac{P_r}{P_t} = \sigma(f)|T(f|^4 \frac{G(f)^2}{4\pi} \times \left(\frac{\lambda}{4\pi R^2}\right)^2$$

brick wall permittivity

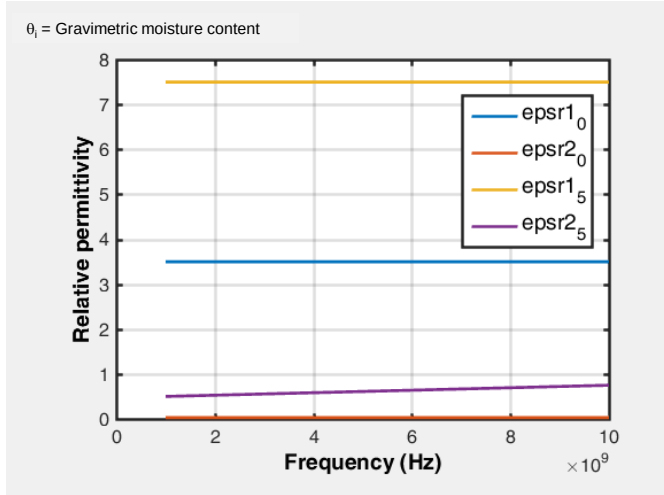

Wall (d = 20 cm) Transmission

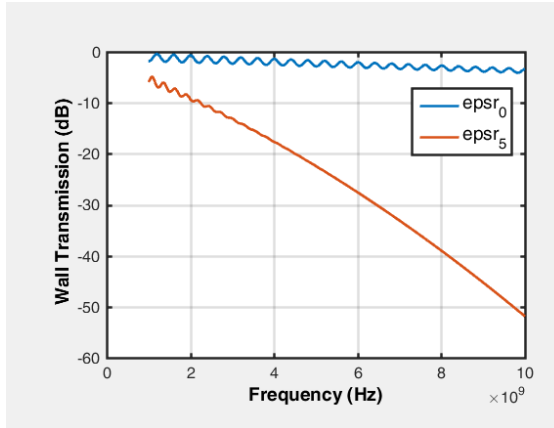

Human body RCS

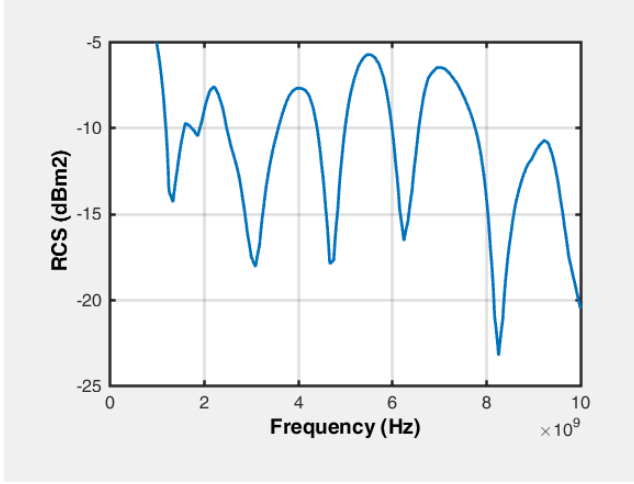

Received power (P_t = 0 dBm, d = 20 cm, R = 10 m)

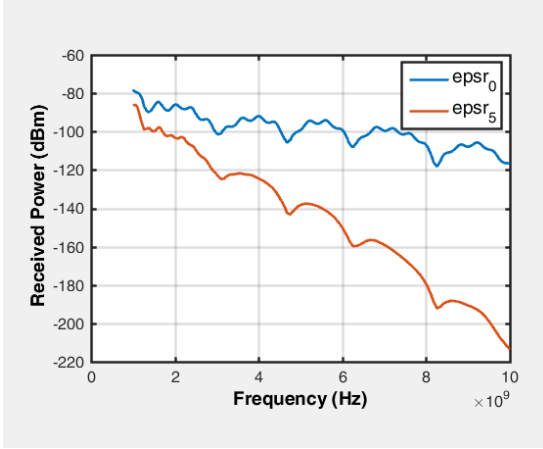

Inversion Problem

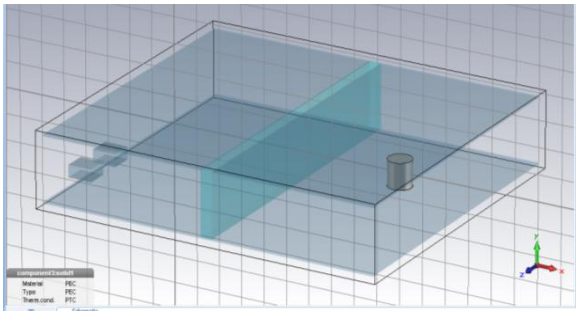

$$I(i,j) = \sum_{k=1}^{Npos} \sum_{l=1}^{Nfreq} S_{21}(l) e^{j\frac{2\pi}{\lambda} d(k)} e^{j\frac{2\pi}{\lambda} \tau_D}$$

Simulation parameters

Truncated waveguide antennas
(a = 18 cm, b = 9 cm)
fc = c/2a = 0.83 GHz

Waveguide distance d = 36 cm

PEC Cylinder
R = 10 cm, h = 20 cm

Wall
d = 15 cm $\varepsilon_r = 4$, $\sigma = 0$

Parameter	Value
Frequency Band B	2 GHz (1 – 3 GHz)
Frequency Step δf	2 MHz
No of frequencies	1001
Non Anbiguous Range (c/δf)	150 m
Pixel Dimension	1 cm x 1 cm
ROI Dimension	200 cm x 300 cm
SAR Aperture (D)	195 cm
array element spacing (S)	7.5 cm = λ/2 at f= 2GHz (Band Centre)
Target Position: Range Cross Range	200 cm 100 cm

Inversion Results

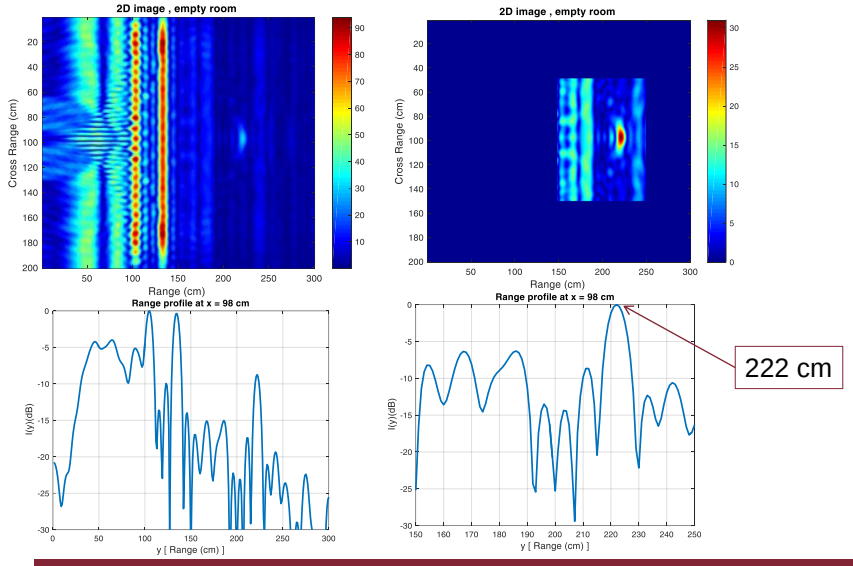

Conclusions

- **Through-the-wall radar imaging systems allows to detect and track humans and moving objects**
- **Design equation and inversion algorithms need the knowledge of wall permittivity values and target RCS**
- **A free-space system suitable for measuring complex permittivity of construction materials (building walls) has been characterized**
- **Tests on different types of walls demonstrated the practical applicability of the system**
- **The complex radar cross section of various target has been evaluated by using a modified semi-anechoic chamber**
- **Theoretical uncertainty figures match well with the experimental ones**
- **A feasibility study evidenced the 1-3 GHz frequency band as the most suitable for TWRI applications**
- **The knowledge of the wall permittivity is mandatory for enhancing imaging accuracy of the TWRI system**

Further developments

- A measurement campaign on a large set of building walls is planned
- Reflection Only techniques will be investigated for wall permittivity measurement
- The RCS of humans and other targets (Guns, rifles, etc.) will be numerically investigated